J Mater Sci (2008) 43:4625–4630
DOI 10.1007/s10853-008-2671-5

Preparation of pH-responsive silver nanoparticles by RAFT polymerization

Youyi Sun · Yaqing Liu · Guizhe Zhao · Xing Zhou · Jiangang Gao · Qijin Zhang

Received: 30 January 2008 / Accepted: 21 April 2008 / Published online: 13 May 2008

Abstract Silver nanoparticles were prepared by chemical reduction of $AgNO_3$ in the presence of the PDMAEMA-*b*-PPA, which was synthesized by the reversible addition-fragmentation transfer technique. The formation of the silver nanoparticles was determined by the transmission electron microscopy (TEM) images and UV–Vis absorption spectra. The average size of the silver nanoparticles was shown to 11.4 nm. Particularly, the pH-responsive property of the silver nanoparticle was further observed. It was characterized by the zate potential, the UV–Vis spectra, and TEM images. The results show that the pH-responsive property is attributed to the aggregate of the silver nanoparticles as a function of pH. The characteristic is expected to apply in the nanoscale optical biosensor and biomaterials.

Introduction

Studies of inorganic nanostructure materials have received much attention due to their unique optical properties and biocompatible characteristics [1, 2]. Especially, the noble nanoparticles are attractive as components in photo and thermally responsive biomaterials for their biocompatible nature and innocuity. Indeed, a specific goal of some research is to develop discrete polymer-coated noble nanoparticles that exhibit structural changes upon exposure to light and thermal polymer and play key roles in a variety of technological applications, including drug delivery, chemical separations and catalysis [3–5]. These polymers readily undergo volume change that is strongly dependent on the lower critical solution temperature [6, 7] as well as other chemical or physical circumstances, such as the solution pH and the nature of the solvent [8, 9].

Meanwhile, the pH-responsive shell/core nanoparticles have been developed to modify a specific physical property of the nanoparticles or to impart pH responsiveness to otherwise unresponsive nanoparticles. At the same time, the pH-sensitive polymers based on zwitterionic copolymers have been particularly well studied [10–13]. But there are few works to investigate the pH-responsive property of the noble nanoparticles grafted with zwitterionic copolymers. It is well known that the silver nanoparticles can be protected by zwitterionic copolymers through the chemosorption of side-chain groups (COO^- or NH^+) on the surface of nanoparticles [14]. However, the pH response is difficult to be observed for the presence of the interaction between the functional ionic groups (COO^- or NH^+) and the noble metal, which restricts the applications of the pH-responsive shell/core nanoparticles on biomaterials.

Taking these into considerations, here a new synthetic approach to prepare zwitterionic copolymers/silver nanocomposite particles has been developed. The key is that the –S– groups are introduced to the zwitterionic copolymer terminus by the reversible addition-fragmentation transfer (RAFT) polymerization as shown in Scheme 1. It is

Y. Sun (✉) · Y. Liu · G. Zhao · X. Zhou
Research Center for Engineering Technology of Polymeric Composites of Shangxi, North University of China, Taiyuan, Shangxi 030051, People's Republic of China
e-mail: syyi@mail.ustc.edu.cn

J. Gao
Department of Biochemistry, Anhui University of Technology and Science, Wuhu, Anhui 241000, China

Q. Zhang
Department of Polymer Science and Engineering, University of Science and Technology of China, Hefei, Anhui 230026, China

Scheme 1 Preparation of the silver nanoparticles in the presence of the PDMAEMA-*b*-PPA

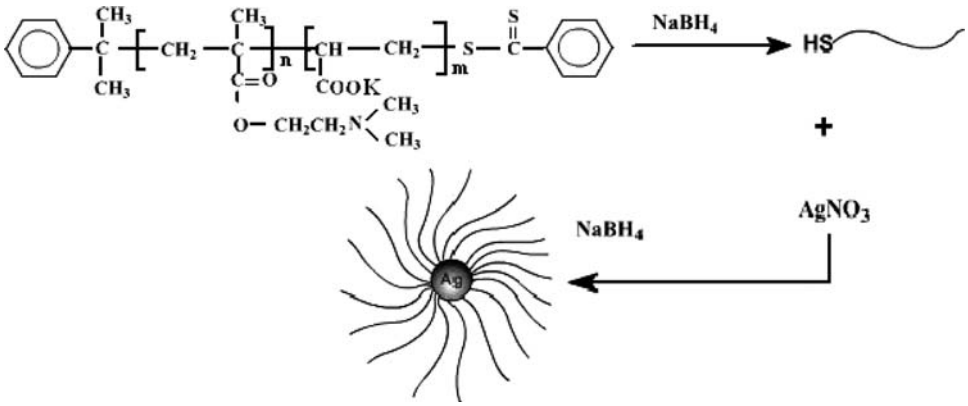

expected to efficiently avoid the interaction between the functional ionic groups (COO^- or NH^+) and the silver nanoparticle because the –S– groups tend to form preferentially σ complexes comparing with other functional groups [15]. It will provide an opportunity to study the pH-responsive property of the silver nanoparticles, which is applied in controlled reversible flocculation, the release of drug and nanoscale optical biosensor.

Experimental sections

Materials

Unless stated otherwise all chemicals were purchased from Aldrich. DMAEMA was purified by passing through a basic alumina column, to remove the inhibitor, stored over CaH_2 at below 0 °C, and distilled immediately prior to use. *S*-benzyl dithiobenzoate (CBD) as the RAFT agent and acrylate kalium was synthesized according to the literature [16] and stored as a solid under vacuum. The polymerization solvent, tetrahydrofuran (THF), was dried over sodium wire prior to reflux over potassium metal for 3 days. This THF was collected by distillation. Other regents were used as received without further purification.

Synthesis of dithioester-terminated PDMAEMA-*b*-PPA

The PDMAEMA was synthesized by RAFT polymerization according to the literature [17]. The PDMAEMA-*b*-PPA was further polymerized by RAFT technique. The RAFT polymerization was conducted in a sealed glass ampule equipped with a magnetic stirring bar. In a typical run, the glass ampule was charged with 1.79 mg of AIBN, 2.0 g of acrylate kalium, 0.5 g of PDMAEMA macroRAFT agent and 5 mL of THF/water (v3:v1) mixing solution used as solvent. The homogenized reaction mixture was subjected to three freeze-thaw cycles to remove oxygen, flame sealed under vacuum and placed in an oil bath at 70 °C for 72 h to complete the polymerization. The polymerization product was precipitated into anhydrous ethyl ether and washed with chloroform for several times to remove residual PDMAEMA monomer. The precipitation-washing cycle was repeated thrice. After purification, the product was dried in a vacuum oven at room temperature overnight.

Preparation of the silver nanoparticles

The silver nanoparticles were prepared by in situ synthetic method as shown in Scheme 1. To a 25 mL round-bottom flask equipped with a magnetic stirring bar, 0.11 g of dithioester-terminated PDMAEMA-*b*-PPA was dissolved in 5 mL deionized water; 5 mL of 32.4 mM $AgNO_3$ aqueous solution was added under vigorous stirring. The mixing mixture was stirred at room temperature for more than 1 h to ensure spread around; a 5 mL of 0.12 M of $NaBH_4$ solution was added dropwise under vigorous stirring. After 4 h of equilibrium at room temperature, the reaction solution was centrifuged at 8000 rpm for 0.5 h and the supernatant was removed. This process removed free polymer chains that were not adsorbed to silver nanoparticles and was repeated thrice. Finally, the silver nanoparticles were obtained, and the pH of silver colloidal solution was further adjusted to 2.5, 8.9 and 12.5 by adding HNO_3 and $NH_3 \cdot H_2O$ aqueous solution.

Characterizations

Nuclear magnetic resonance (NMR) spectroscopy

All ^{1}H-NMR spectra were recorded using a Bruker 300 MHz spectrometer. PDMAEMA macroRAFT agent and PDMAEMA-*b*-PPA were analyzed in $CDCl_3$ and D_2O, respectively.

UV–Vis spectra were acquired on a Unico UV–Vis 2802PCS spectrophotometer.

Transmission electron microscopy

Transmission electron microscopy (TEM) observations were conducted on a Philips CM 120 electron microscope at an acceleration voltage of 100 kV. The sample for TEM observations was prepared by placing drop of hybrid copolymer and silver nanoparticle solution on copper grids coated with thin films of Formvar and carbon successively. No staining was required.

Zeta potential as function of pH was conducted on zeta potential measurements (ZETAPHOREMETER IV), in which they were carried out in 100 mmol NaCl solutions in order to keep a constant electrical double layer.

Results and discussion

Synthesis of the PDMAEMA-*b*-PPA by RAFT technique

The MacroRAFT agent PDMAEMA and the PDMAEMA-*b*-PPA were prepared by a general approach of RAFT polymerization [17]. Costas et al. have investigated the RAFT polymerization using PDMAEMA marcoRAFT agent and stated that the polymerization can be carried out in a controlled manner [17, 18]. So, here we did not study in detail the kinetics of RAFT polymerization. Figure 1A shows the structure of the PDMAEMA marcoRAFT by the ^{1}H-NMR, such as b (4.2–4.4 ppm, 2H), c (2.7–2.9 ppm, 2H), d (2.4–2.6 ppm, 6H), e (1.9–2.1 ppm, 2H), and f (0.9–1.1 ppm, 3H), which are consistent with the result of previous work [17]. Furthermore, the characteristic signal of –CH– of phenyl at 7.5 ppm is observed, indicating that the –S– group is introduced into the PDMAEMA terminus by the RAFT technique. The structure of the dithioester-terminated PDMAEMA-*b*-PPA is also confirmed by the H^1-NMR as shown in Fig. 1B. It shows the characteristic signals of the PPA block at δ1.2–1.4 and δ2.1–2.3 besides the characteristic signals (b–f) of PDMAEMA block. The molecular weight and molecular weight distribution of the PDMAEMA-*b*-PPA are characterized by gel permeation chromatography (GPC), resulting in M_n of 19,800 and M_w/M_n of 1.15. The relatively narrow distribution of the molecular weight further indicates that the PDMAEMA-*b*-PPA is synthesized by the "living" character of the RAFT polymerization, which also reveals the presence of –S– group on the PDMAEMA-*b*-PPA terminus [19].

Preparation of the silver nanoparticles

The silver nanoparticles were prepared by reducing $AgNO_3$ with NaH_4B in the presence of the PDMAEMA-*b*-PPA. The formation of the silver nanoparticles is confirmed by the UV–Vis absorption spectrum and TEM image as shown in Fig. 2. The strong absorbing band of 405.0 nm (Fig. 2a) is attributed to surface plasmons resonance absorption of the silver nanoparticles, which confirms the formation of the silver nanoparticles [20]. At the same time, the narrow absorbing band suggests the size of silver nanoparticles with a monodispersion. The typical bright field TEM image and histogram of the size distribution are shown in Fig. 2b, c for the sample, respectively. The image shows that all the particles are almost spherical and the mean diameter is about 11.4 nm. The narrow size distribution further indicates the monodispersion of silver nanoparticles' size. The mean diameter and size distribution are obtained by counting at least 100 particles in the sample. Approximately spherical nanoparticles should be ascribed to the silver core. The diblock copolymer monolayer cannot be observed under TEM observation. The preparation of PNIPAM and PS polymers protected silver nanoparticles has been reported in previous works [11, 21]. They also did not observe the polymer layer by TEM. This is attributed to that the monolayer of PDMAEMA-*b*-PPA may be too thin in the dry state to be clearly discerned under TEM observation. The silver nanoparticles can stably remain in aqueous solution for at least 2 months, indicating that the silver nanoparticles are protected by the polymer molecules of the PDMAEMA-*b*-PPA.

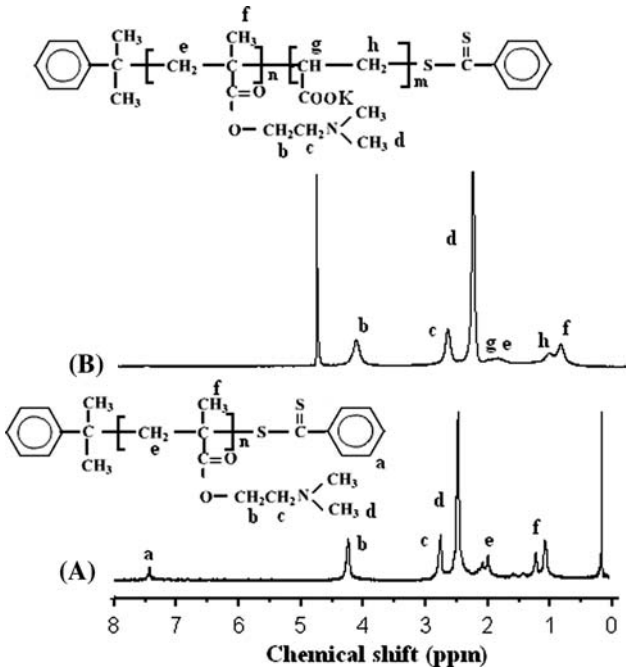

Fig. 1 H^1-NMR spectra of (**a**) PDMAEMA and (**b**) PDMAEMA-*b*-PPA in CD_3Cl and D_2O, respectively (400 Hz)

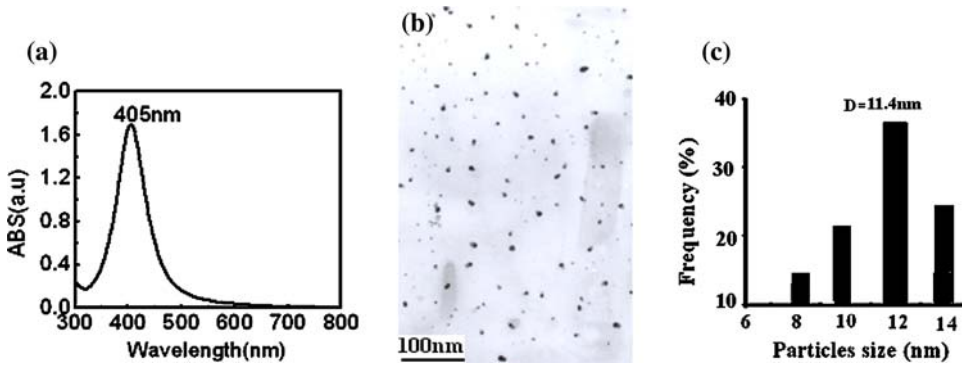

Fig. 2 (**a**) UV–Vis spectrum, (**b**) TEM image, and (**c**) size distribution of the silver nanoparticles

Figure 3 shows the FT-IR spectra of the PDMAEMA-*b*-PPA and the silver nanoparticles. IR absorbing band of the silver nanoparticles from 4,000 to 500 cm^{-1} (Fig. 3b) is attributed to the organic PDMAEMA-*b*-PPA because the silver nanoparticles have no any absorption in this range [22], suggesting that the PDMAEMA-*b*-PPA is anchored on the surface of the silver nanoparticles. The absorbing bands of 1,726.2 and 1,141.3 cm^{-1} as shown in Fig. 3a are assigned to the stretching mode of the C=O and the C–N groups, respectively. An observation of the spectrum (Fig. 3b) shows that the C=O and the C–N stretching frequencies is almost no-change after the adsorption of PDMAEMA-*b*-PPA on the silver nanoparticles. The result suggests that there is no any interaction between the silver and the C–N or the C=O groups, which is different from previous works [23, 24]. And here it is thought that the silver nanoparticles are coated with PDMAEMA-*b*-PPA through the interaction between the silver and the terminus groups –S– of the copolymer, which is consistent with the literature [15].

pH-Responsive property of the silver nanoparticles

The zeta potential of the silver colloidal solution (0.01 wt%) has been measured as a function of pH as shown in Fig. 4. The zeta potential of the silver colloidal solution decreases with increasing in the solution pH. At the same time, an IEP of the silver colloidal solution at pH 8.9 is observed. According to the literature [25], the zeta potential of the silver colloidal solution as a function of pH is attributed to the diblock copolymer of PDMAEMA-*b*-PPA adsorbing on surface of the silver nanoparticles. Compared with previous works [11, 25], the higher IEP is obtained in this case due to the increased proportion of DMAEMA residues in the copolymer. At pH smaller than the IEP, the zwitterionic copolymer of PDMAEMA-*b*-PPA has a net positive charge. At the IEP, the net charge is zero, resulting from charge neutralization between the COO^- and the NH^+ groups. And then it turns to a negative value at pH higher than the IEP, as shown in Fig. 4. At and above the IEP, the copolymer becomes insoluble, resulting in an aggregate of the silver nanoparticles. This is thought to

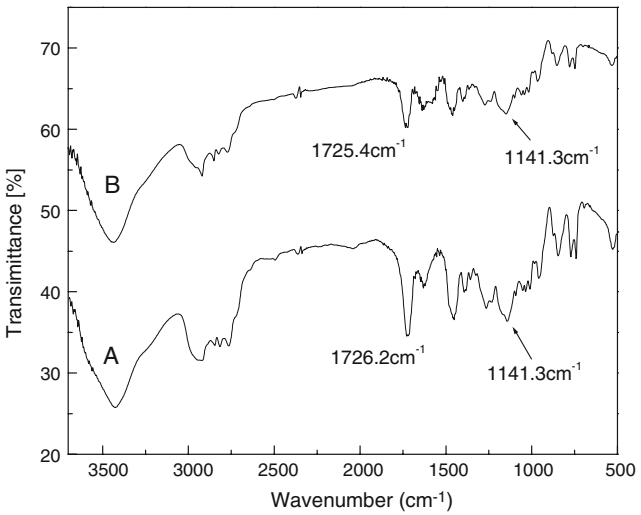

Fig. 3 FT-IR spectra of (**a**) the PDMAEMA-*b*-PPA and (**b**) the silver nanoparticles

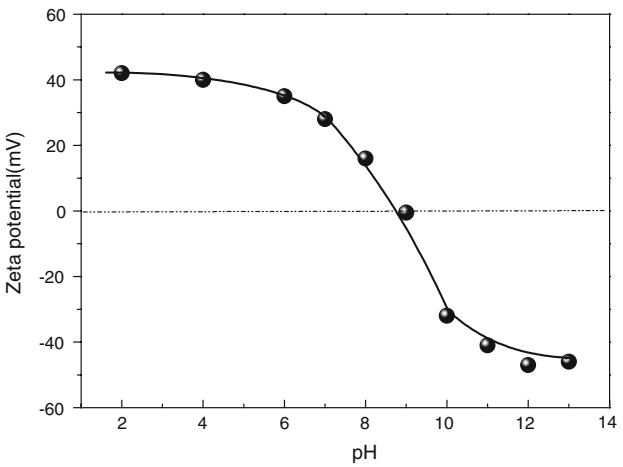

Fig. 4 Zeta potential versus pH curves obtained for the diblock copolymer of PDMAEMA-*b*-PPA

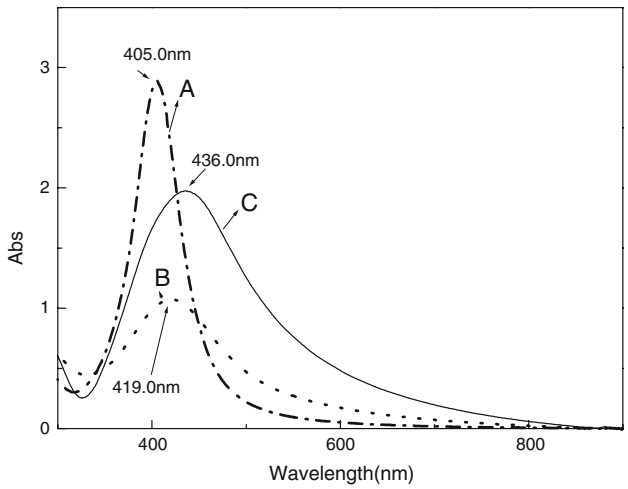

Fig. 5 UV–Vis absorption spectra of the silver nanoparticles in aqueous solution with various pHs of (**a**) 2.5, (**b**) 8.9, and (**c**) 12.5

result from hydrophobic interactions between uncharged PDMAEMA blocks that render the copolymer insoluble.

Figure 5 shows the surface plasmons resonance absorption bands of the silver colloidal solution as a function of pH. It shows that the characteristic surface plasmons resonance absorption peak' position increases with increasing in solution pH. The absorbing peak at 405.0 nm is red shift to 419.0 and 436.0 nm at elevating the pH from 2.5 to 8.9 and 12.5, respectively. At the same time, the absorbing band is relatively broadened with increasing in pH value. According to the literatures [26, 27], the surface plasmons resonance absorption peak and width are determined by the size and the shape of particle, the properties of surround and surface environment, and the aggregate of particles. So, here these results are attributed to the aggregate of the silver nanoparticles, resulting in scattering of light [26, 28, 29]. The silver nanoparticles trend to aggregate at and above IEP (pH = 8.9), resulting

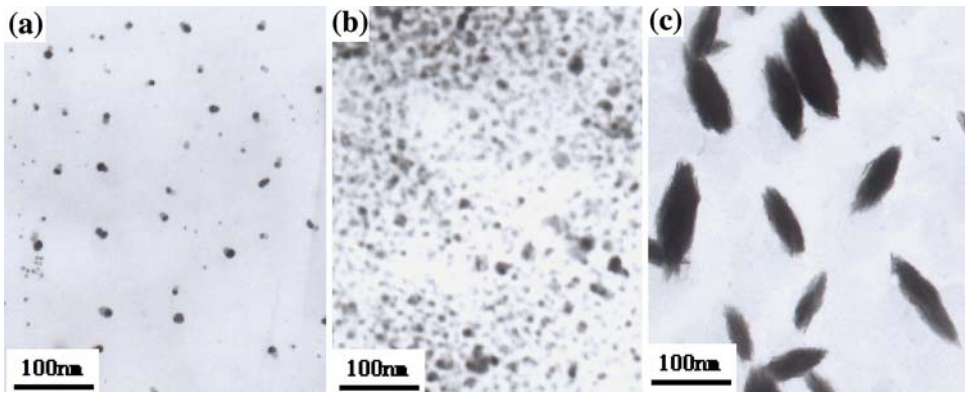

Fig. 6 TEM images of silver nanoparticles in aqueous solution with various pHs of (**a**) 2.5, (**b**) 8.9, and (**c**) 12.5

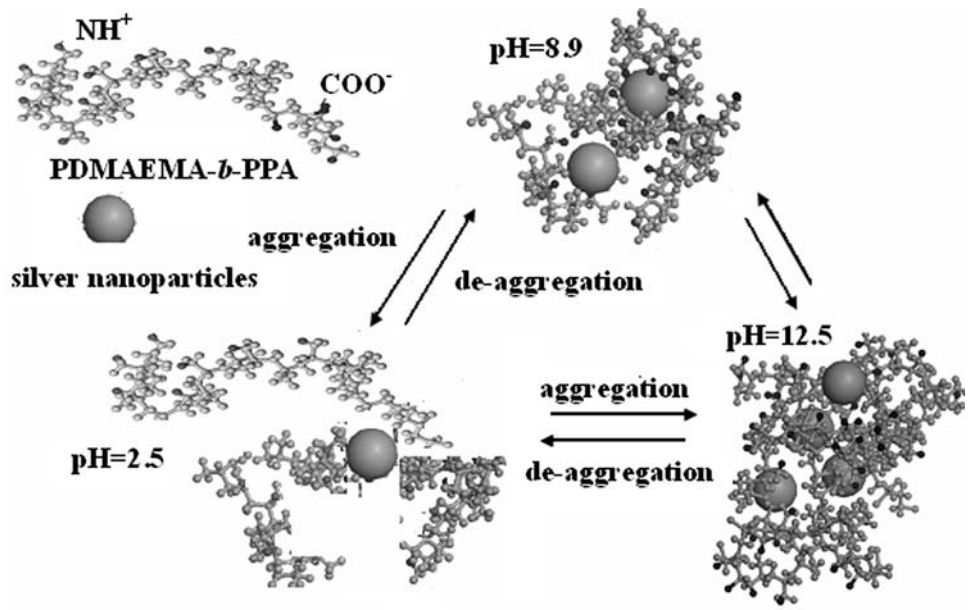

Scheme 2 Representation of the aggregate and de-aggregate of the silver nanoparticles at various pHs value

from the insolubility of the PDMAEMA-*b*-PPA in aqueous solution, which has been discussed above in Fig. 4.

The assignment of the shifted absorption band to aggregate species is supported by the observation of TEM images as shown in Fig. 6. It clearly shows the presence of large and multi-particle aggregates at pH of 8.9 and 12.5 comparing with pH of 2.5. The average sizes are about 22 nm and 110 × 45 nm^2 as shown in Fig. 6b, c, respectively. Furthermore, the silver nanorod can simply be obtained by the aggregate of the silver nanoparticles at pH of 12.5, which is a novel synthetic method for the preparation of the silver nanorod.

Importantly, the pH-induced aggregate of the silver nanoparticles is reversible if the pH is lower than IEP within a period of hours after aggregate. The mechanism for aggregate and de-aggregate is shown in Scheme 2. The forces which favor aggregate of the copolymer at and above IEP (pH = 8.9 and 12.5) are the combination of electrostatic interactions between the $–COO^-$ and the $–NH^+$, and hydrophobic interaction between uncharged PDMAEMA blocks. These interactions may not be any stronger than the soluble interactions, but the copolymer can form many of these bonds with one another. Contrarily, at pH smaller than IEP (pH = 2.5), the driving force for aggregation may be overcome by intense coulombic repulsion caused by the multiple positive charges residing on each PDMAEMA and hydrophilic action of PDMAEMA. So, de-aggregate is easy to happen for these silver nanoparticle aggregates.

Conclusions

The PDMAEMA-*b*-PPA copolymer was synthesized by the RAFT technique, which was confirmed by H^1-NMR and GPC analysis. The silver nanoparticles were further prepared by in situ synthetic method in the presence of the PDMAEMA-*b*-PPA. The average size of these nanoparticles was about 11.4 nm according to the TEM image analysis. The IR spectrum of the silver nanoparticles shows that the PDMAEMA-*b*-PPA adsorbs to the surface of silver nanoparticles by the interaction between the silver and the terminus groups –S– of the polymer. Furthermore, the pH-responsive property of the silver nanoparticles was further observed, resulting from aggregate and de-aggregate of the silver nanoparticles grafted with PDMAEMA-*b*-PPA. The characteristic property of the silver nanoparticles is expected to apply in a nanoscale optical biosensor as a function of solution pH.

Acknowledgements This work was supported by the Natural Science Foundation of Shangxi (Nos. 033004 and 200671037), Youthful Science Foundation of Shanxi province (Nos. P20072185 and P20072194), and the Youthful Science Foundation of North university. The authors are grateful for the financial support and express their thanks to Zhang Zhiyi for helpful discussions and Gao jinfeng for FT-IR measurements.

References

1. Noritsugu K, Makoto T, Takeshi F, Kenji A, Yoshiro Y (2001) Langmuir 17:578. doi:10.1021/la0013190
2. Yuzhen S, Jacek S, Tzu-Chau L, Przemyslaw M, Paras NP (2002) J Phys Chem B 106:4040. doi:10.1021/jp014639g
3. Pelton R (2000) Adv Colloid Interface Sci 85:1. doi:10.1016/S0001-8686(99)00023-8
4. Jeong B, Bae YH, Lee DS, Kim SW (1997) Nature 388:860. doi:10.1038/42218
5. Bergbreiter DE, Case BL, Liu YS, Caraway JW (1998) Macromolecules 31:6053. doi:10.1021/ma980836a
6. Jun S, Jie C, Markus N, Tapani V, Hua J, Jouko P, Esko K, Heikki T (2006) Langmuir 22:794. doi:10.1021/la052579q
7. Zhu MQ, Wang LQ, Gregory JE, Alexander DQ (2004) J Am Chem Soc 126:2656. doi:10.1021/ja038544z
8. Sang YP, You HB (1999) Macromol Rapid Commun 20:269. doi:10.1002/(SICI)1521-3927(19990501)20:5<269::AID-MARC269>3.0.CO;2-3
9. Youngjin K, Robert CJ, Joseph TH (2001) Nano Lett 1:165. doi:10.1021/nl0100116
10. Sean B, Dyer N, Anthony G (2003) Biomacromolecules 4:1224. doi:10.1021/bm034048r
11. Bütün V, Lowe AB, Billingham NC, Armes SP (1999) J Am Chem Soc 121:4288. doi:10.1021/ja9840596
12. Jean-François G, Serge C, Myriam G, Boris M, Manfred S, Jérôme R (2000) Macromolecules 33:6378. doi:10.1021/ma992016j
13. Jean-François G, Sayed A, Jérôme R (2001) Macromolecules 34:7435. doi:10.1021/ma010535s
14. Evgenii BB, Dmitry AP, Marina VB (2004) Langmuir 20:10868. doi:10.1021/la048601h
15. Jacob WC, Michael PS, James MT (2004) J Am Chem Soc 126:13172. doi:10.1021/ja0472477
16. Peng QL, Doreen MYE, Kang T, Neoh KG (2006) Macromolecules 39:5577. doi:10.1021/ma0607362
17. Zhao Q, Peihong N (2005) Polymer 46:3141. doi:10.1016/j.polymer.2005.01.089
18. Costas SP, Leo RS, Steven PA, Norman CB (1999) Langmuir 15:1613. doi:10.1021/la970662a
19. Mayadunne RTA, Rizzardo E, Chiefari J, Krstina J, Moad G (2000) Macromolecules 33:243. doi:10.1021/ma991451a
20. Callegari A, Tonti D, Chergui M (2003) Nano Lett 3:1565. doi:10.1021/nl034757a
21. Cliffel DE, Zamborini FP, Gross SM, Murray RW (2000) Langmuir 16:9699. doi:10.1021/la000922f
22. Sun YY, Wang D, Gao JG, Zheng Z, Zhang QJ (2007) J Appl Polym Sci 103:701
23. Dongshan Z, Liang L, Gi X (2002) Langmuir 18:4559. doi:10.1021/la025611e
24. Zhou JL, Yang JJ, Sun YY, Zhang DG, Zhang QJ (2007) Thin Solid Films 515:7242. doi:10.1016/j.tsf.2007.02.091
25. Gohy JFo, Creutz S, Garcia M, Mahltig B (2000) Macromolecules 33:6378. doi:10.1021/ma992016j
26. Sooklal K, Hanus LH, Ploehn H, Murphy JC (1998) J Adv Mater 10:1083. doi:10.1002/(SICI)1521-4095(199810)10:14<1083::AID-ADMA1083>3.0.CO;2-B
27. Storhoff JJ, Lazarides AA, Mucic RC, Mirkin CA, Letsinger RL, Schatz GC (2000) J Am Chem Soc 122:4640. doi:10.1021/ja993825l
28. Zheng J, Stevenson MS, Hikida RS, Van Patten PG (2002) J Phys Chem B 106:1252. doi:10.1021/jp013108p
29. Lazarides AA, Schatz GC (2000) J Phys Chem B 104:460. doi:10.1021/jp992179+